Preparation and Electrochemical Studies of Layered PANI/HNb_3O_8 Nanocomposite

Gang Yang,[1,2] Yuge Liu,[1] Wenhua Hou,[1] Hongmei Ji,[2] Yuhong Li[2]

[1]*Laboratory of Mesoscopic Chemistry of MOE, School of Chemistry and Chemical Engineering, Nanjing University, Nanjing 210093, People's Republic of China*
[2]*Jiangsu Laboratory of Advanced Functional Material, Department of Chemistry, Changshu Institute of Technology, Changshu 215500, People's Republic of China*

Received 28 November 2007; accepted 15 December 2008
DOI 10.1002/app.29907
Published online 13 March 2009 in Wiley InterScience (www.interscience.wiley.com).

ABSTRACT: Aniline monomers could be easily inserted into and polymerized within the interlayers of HNb_3O_8. The conformation and electrochemical properties of the resulting nanocomoposites were discussed in detail. Two different mechanisms were proposed for the polymerization of monomers within the confined interlayers initiated by chemical oxidants and microwave irradiation, respectively. The analyses of thermogravimetric/differential scanning calorimetric analyses, X-ray diffraction, and Fourier transform infrared spectra indicated that the aromatic rings of the interlayered polyaniline (PANI) could be parallel with or perpendicular to the inorganic slabs, and the interlayered PANI molecules were emeraldine salt and protonated by the protons of layered inorganic acid host. The cyclic voltammetry revealed that the properties of the layered host and the interlayer height have an effect on the redox behavior of the corresponding nanocomposites. Compared with the nanocomposites in which the aromatic rings were parallel with the inorganic slabs, the nanocomposites in which the aromatic rings were perpendicular to the slabs demonstrated a higher conductivity and electrochemical activity. © 2009 Wiley Periodicals, Inc. J Appl Polym Sci 113: 78–86, 2009

Key words: nanocomposite; intercalation; conducting polymer; layered niobic acid; electroactivity

INTRODUCTION

By the intercalation technique, organic guest can be inserted into and combined with inorganic host material on nanoscale (~ 10 Å), resulting in the formation and modification of nanocomposite materials.[1] These nanocomposites have a high potential for advanced electronic, magnetic, optical photonic, and chemical sensing applications.[2] When the polymerization is initiated between the layers, where the slabs of the inorganic host serve as a template, a relatively ordered arrangement of polymer molecules can be formed within the confined environment.[3] Several kinds of polymers, such as polyethylene oxide, polypyrrole, and polyaniline (PANI), have been intercalated into different layered materials by using a variety of insertion and polymerization methods.[3,4] The resulting lamellar nanocomposites demonstrate some novel properties such as photonic, chemical sensoring, and electrochemical properties, which are not possible for a single component separately.[4,5]

Nanocomposites based on PANI are of particular interest. These materials are currently being investigated for applications in organic batteries, biosensors, color displays, microelectronic devices, sensors, etc.[6–9] PANI is a promising conductive polymer with interesting electrical properties. Emeraldine base (EB) PANI can be converted from insulator (undoped form) to conductor (doped form) by the local modification (e.g., simple protonation) of the chemical structure.

The exact chemical structure of PANI molecule is still fragmentarily known because of the amorphous or poor crystalline nature and the insolubility of PANI in common solvents. MacDiarmid and coworkers once studied the microcrystalline form of PANI and proposed a crystal structure.[8] To obtain oriented polymer chains, the polymer molecules were forced to grow inside the structurally organized three-dimensional hosts with large oriented

Correspondence to: W. Hou (whou@nju.edu.cn).
Contract grant sponsor: National Natural Science Foundation of China; contract grant number: 20773065.
Contract grant sponsor: National Basic Research (973) Program of China; contract grant number: 2007CB936300.
Contract grant sponsor: Natural Science Foundation of Jiangsu Province of China; contract grant number: BK2006537.
Contract grant sponsor: Natural Science Foundation of Jiangsu Educational Department of China; contract grant number: 06KJA43014.
Contract grant sponsor: Modern Analysis Center of Nanjing University.

tunnels and two-dimensional ones with an interlayer space.[10–17] Recently, Petkov et al.[10] studied the three-dimensional structure of PANI/V_2O_5 nanocomposite by using the technique of atomic pair distribution function. Their results directly yield three-dimensional structural information for materials of limited structural coherence, including nanostructured materials and organic/inorganic hybrids, and thus provide a way for better explaining, predicting, and possibly improving the properties of these materials.

Compared with the bulk PANI, the strong intermolecular interaction of PANI molecules is decreased by the inorganic slabs when PANI is formed between the layers. In these PANI/layered inorganic compound nanocomposites, some key problems such as the molecular structure and properties of the interlayered PANI are still open. The degree of oxidation and doping level are the most important factors that can affect the electrochemical properties of PANI. Many investigations have been carried out on the preparation, structures, and properties of bulk PANI with different oxidation and doping states.[18] MacDiarmid and coworkers systematically investigated the change of electric conductivity in PANI doped by protonic acid.[19] They reported the variation of conductivity as a function of HCl concentration for emeraldine salt (ES) prepared by electrochemical and chemical methods. When the aniline monomers are inserted into inorganic layered materials and are then polymerized between the layers, the two dissimilar chemical components can be combined at a molecular level. It is advantageous to understand the electrochemical properties of nanocomposites by studying the chain structure and polymerization mechanism of PANI formed within the layers.

Because of the particular layer properties, layered protonic transition metal oxides have been extensively studied as fast ion conductors, catalysts, potential electrode materials, and so on.[20] They are typically synthesized as alkaline metal-containing layered oxides, consisting of polyhedral sheets of transition metal oxides with intercalated alkaline metal cations. The interlayered alkaline metal cations could be replaced by various other cations through ion-exchange reactions.[21] In general, the negative charge density of layered transition metal oxides is higher than that of other layered compounds such as the most extensively studied clay minerals, and the sheets of the material often exhibit conductivity and photo responses based on band gap transitions. These layered materials offer several attractive features. For example, the H^+-exchanged form of the layered transition metal oxides exhibits a strong acidity. The layered compound HNb_3O_8 is a relatively strong Brønsted acid and has been the focus in the field of semiconductor and photochemical catalysis.[20,22] The acidic layered HNb_3O_8 material, where H^+ ions are placed between 2D negative sheets composed of NbO_6 octahedra, also exhibits a distinct intercalation behavior toward organic molecules.

Here, we describe a different approach in which aniline monomers were first inserted into the interlayer of HNb_3O_8 based on the force of acid/base reaction, and then the novel nanocomposites PANI/HNb_3O_8 were synthesized through the polymerization initiated by microwave irradiation and chemical oxidants, respectively. The interlayered PANI molecules were doped by the host protons. A detailed characterization and studies of the structure, polymerization mechanism, and electrochemical properties of these nanocomposites are presented.

EXPERIMENTAL SECTION

Synthesis of layered solid acid and monomer composite

HNb_3O_8 was prepared from KNb_3O_8 powders according to the procedure described in the literature.[23] The proton-exchange reaction of KNb_3O_8 in strong inorganic acid at room temperature gave the corresponding layered acidic material HNb_3O_8. HNb_3O_8 (3 g) was first dispersed in 60 mL distilled water, and then 3 mL aniline was added into the HNb_3O_8 aqueous solution. The acid/base reaction of the aniline with the protons of layered host was the main driving force of the intercalation. The mixture was stirred for 2 days at room temperature. The monomer-intercalated product (denoted as AnHNb) was filtered, washed thoroughly with distilled water and absolute ethanol for several times until the UV spectrum of the washed solution did not present any peaks of pure aniline. The obtained product was finally dried at room temperature in vacuo.

Polymerization of the intercalated monomers between the layers

The polymerization of the intercalated aniline monomers was explored by two methods*. (i) The monomer composite was treated with microwave irradiation at the power of 600 W for 2 h. The sample color changed from yellow to gray-black. The nanocomposite PANI/HNb_3O_8 was obtained and simply denoted as PANIHNb-MW. (ii) The monomer composite was treated with two different oxidants $(NH_4)_2S_2O_8$ and $FeCl_3$, respectively, in an ice bath for 24 h, and the sample color turned to dark-green and greenish-blue, respectively. The

*The monomer composite of aniline/HNb_3O_8 was also heated at 130°C for 2 days, but the polymerization did not occur, only one layer of aniline within the layers was lost as confirmed by XRD, IR, and TGA measurements.

precipitate was filtered, washed with distilled water and ethanol for several times, and finally dried at 40°C in vacuo. The obtained two nanocomposites were simply denoted as PANIHNb-NH_4^+ and PANIHNb-Fe^{3+}, respectively.

Characterization

Thermogravimetric and differential scanning calorimetric analyses (TGA/DSC) were performed with a Shimadzu TGA-50 under a nitrogen flow of 30 mL min^{-1}, and the measurements were conducted from room temperature to 800°C at a heating rate of 10°C min^{-1}. The change of basal spacing during monomer intercalation and subsequent polymerization was confirmed by X-ray powder diffraction (ARL X'TRA X-ray diffractometer (Waltham, MA), Ni-filtered, and Cu Kα radiation). A continuous scanning mode with a speed of 1° min^{-1} and an increment of 0.05° in 2θ was chosen. Fourier transform infrared spectra (FTIR) were obtained at room temperature on a Bruker Vector 22 FTIR spectrometer (Billerica, MA) using pressed KBr pellets. Scanning electron microscopy (SEM) and transmission electron microscopy (TEM) were done with Hitachi (Tokyo, Japan) X650 microscope (20 kV) and JEOL JEM-200CX (200 kV).

Electrochemical studies

Cyclic voltammetry (CV) were performed in a conventional electrochemical cell at room temperature. The glassy carbon electrodes (GCE, 3 mm in diameter) were polished with 1.0, 0.3, and 0.05 μm alumina slurry followed by rinsing with doubly distilled water and drying at room temperature. The obtained nanocomposite was dispersed in distilled water to form a 1.0 mg mL^{-1} solution and ultrasonically treated for 30 min. The colloidal solution (5 μL) was dropped onto the pretreated GCE surface and allowed to dry under ambient conditions. For each value reported, at least three measurements were averaged. Electrochemical experiments were conducted with an Autolab PGSTAT 30 system (Ecochemie, Utrecht, The Netherlands). All electrochemical experiments were performed in a cell containing 20.0 mL of HCl solution with different pH values at room temperature, using a coiled platinum wire as the auxiliary electrode, a saturated calomel electrode as the reference electrode, and the nanocomposite PANI/HNb_3O_8-modified electrode as the working electrode.

RESULTS AND DISCUSSION

Thermogravimetric analysis of nanocomposites

Figure 1 presents TGA/DSC curves of HNb_3O_8, bulk PANI, AnHNb, PANIHNb-NH_4^+, PANIHNb-Fe^{3+}, and PANIHNb-MW. The TGA/DSC curve of AnHNb exhibits four principal weight losses [Fig. 1(b)]. The first weight loss at the temperature range of 100–200°C is due to the partial evaporation of aniline from the HNb_3O_8 layers (about 11 wt %), which can be confirmed by the decrease of interlayer spacing from 21.34 to 16.34 Å in XRD patterns after heating AnHNb at the same temperature range. The second weight loss (about 1.6 wt %) can be assigned to the dehydration of the host HNb_3O_8, which is similar to that of pure HNb_3O_8 [Fig. 1(a)] and presents an endothermic peak at 318°C. The last two endothermic weight losses at the temperature range of 395–600°C resulted from the decomposition of the interlayered aniline. These last two weight losses have a sum of ~ 11.3 wt %. Such a value suggests that there is only one monolayer of aniline molecules remaining within the interlayer of HNb_3O_8 after the first and second weight losses, rather than a bilayer of aniline molecules for the as-synthesized AnHNb (also see XRD).

Figure 1(c) displays TGA/DSC curve of nanocomposite PANIHNb-NH_4^+. The absence of weight loss at the temperature range of 100–200°C indicates that there is no aniline monomer between the layers after polymerization. The weight loss near 315°C is due to the dehydration of HNb_3O_8, it is accompanied with an endothermic peak. The weight loss (ca. 9 wt %) accompanied with two endothermic peaks at the temperature range of 400 and 620°C corresponds to the decomposition of PANI molecules with different molecular weights between the layers. By comparison, bulk PANI prepared by chemical polymerization shows degradation in a relatively wider temperature range, indicating that the PANI within HNb_3O_8 layers may have a much narrower molecular weight distribution than bulk PANI.

The TGA/DSC curves of the other two nanocomposites PANIHNb-Fe^{3+} and PANIHNb-MW are similar to those of PANIHNb-NH_4^+. At the temperature range of 400–600°C, the weight losses of PANIHNb-Fe^{3+} and PANIHNb-MW are about 8.7 and 3.9 wt %, respectively.

X-ray powder diffraction and conformation of PANI within the confined layers

HNb_3O_8 shows a relatively strong Brønsted acidity and is an ideal 2D host. Some basic monomers, such as aniline, can be inserted and then polymerized to form PANI molecules between the layers. Scheme 1 shows a schematic representation of the process, and Figure 2 shows the powder XRD patterns of the starting materials and obtained nanocomposites. Upon intercalation, the characteristic reflection peak of the layered compound is shifted toward a lower 2θ angle. Since the interlayer distance of KNb_3O_8 is

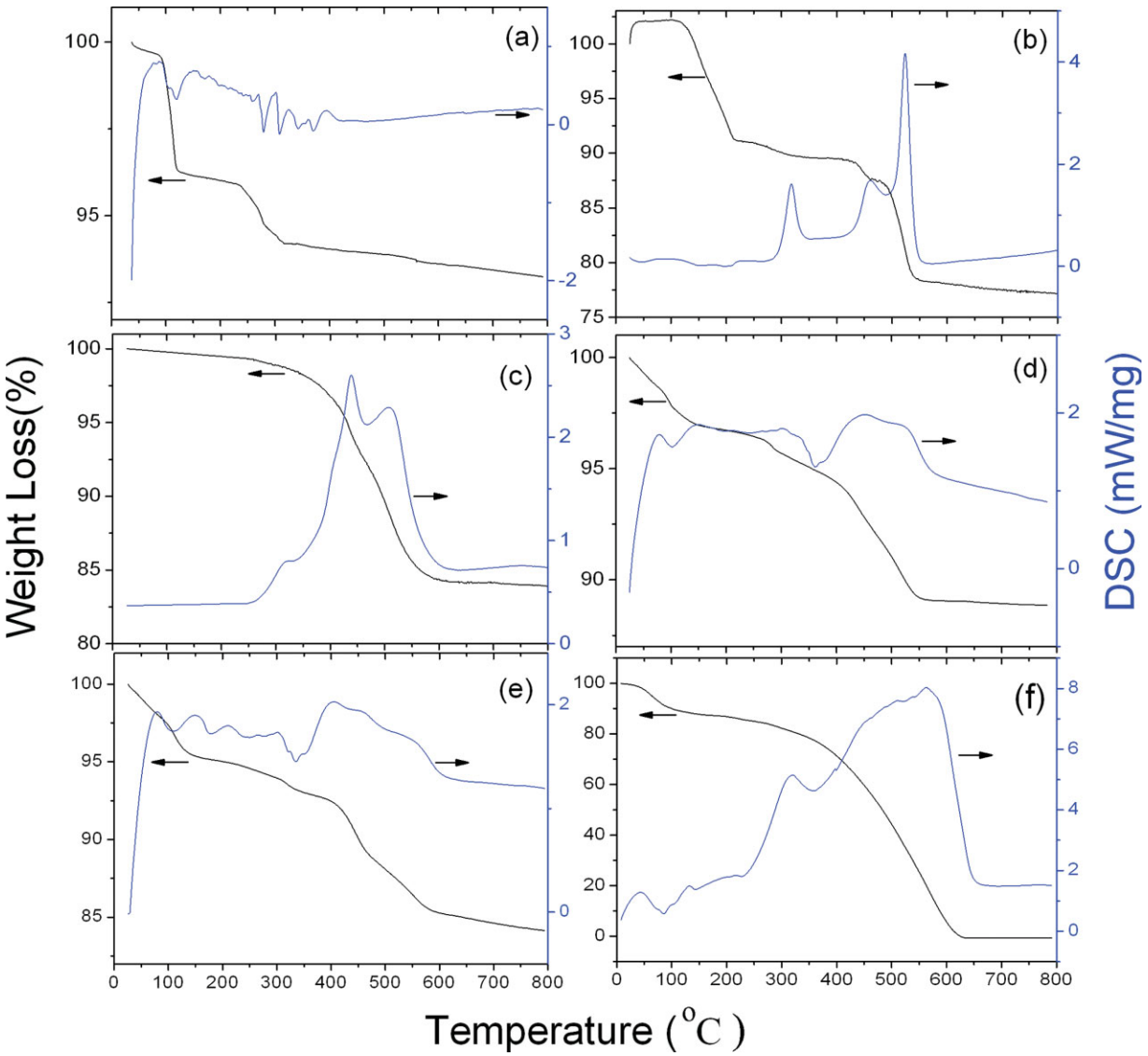

Figure 1 TGA/DSC curves of (a) HNb_3O_8, (b) AnHNb, (c) PaniHNb-NH_4^+, (d) PaniHNb-Fe^{3+}, (e) PaniHNb-MW, and (f) bulk PANI. [Color figure can be viewed in the online issue, which is available at www.interscience.wiley.com.]

10.54 Å, the thickness of $Nb_3O_8^-$ slab is calculated to be 8.14 Å by subtracting the diameter (~ 2.4 Å) of the interlayered K^+ ions. As shown in Figure 2(c), the monomer composite AnHNb has an interlayer distance of 21.34 Å. By subtracting the thickness (8.14 Å) of $Nb_3O_8^-$ slab, the net interlayer height is 13.2 Å. A similar expansion of ~ 12Å, corresponding to the formation of a bilayer arrangement of aniline monomers within the layers (Scheme 1, left), was also observed in layered V_2O_5, zirconium phosphonate, and so on.[11,24]

Being initiated by oxidant $(NH_4)_2S_2O_8$, the interlayered aniline monomers will be polymerized to form PANI. As shown in Figure 2(d), the net interlayer height of the as-prepared nanocomposite PANIHNb-NH_4^+ is decreased from 13.2 Å to 7.3 Å. Such a change can be used to suggest that a single-layer arrangement of PANI molecules is formed within the layers, and the idealized representation is shown in Scheme 1 (right). During the polymerization, some aniline molecules are exchanged away by the other ions and form soluble oligomers. Similar results were also revealed in the polymerization of AnHNb initiated by chemical oxidant $FeCl_3$ or microwave irradiation[†], but the net interlayer heights of nanocomposites PANIHNb-Fe^{3+} and PANIHNb-MW are 4.4 and 7.4 Å, respectively. These expansions are also corresponding to the formation of a single-layer arrangement of PANI molecules

[†]During the polymerization initiated by microwave irradiation, the monomer composite AnHNb could achieve more than 70°C in microwave field for 2 h because of the heat produced by the polymerization and microwave irradiation. As a result, some aniline monomers were evaporated from the interlayer of AnHNb.

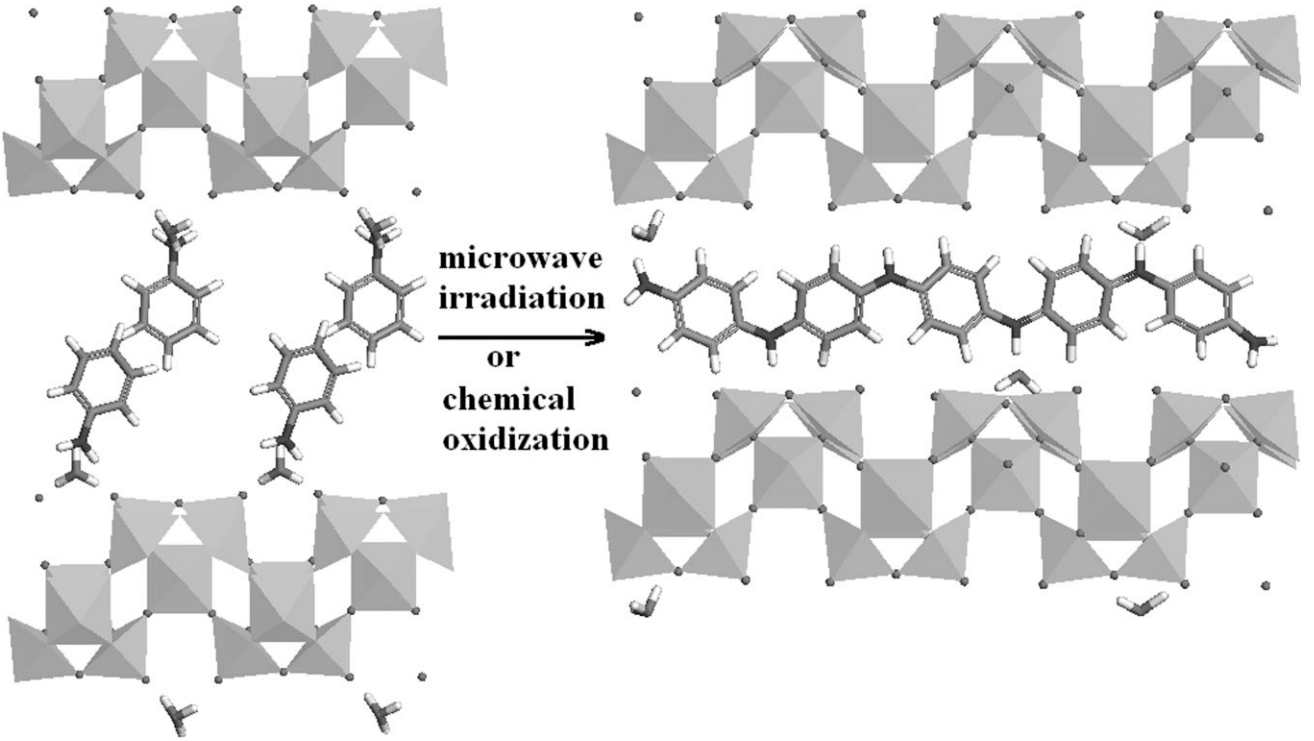

Scheme 1 Schematic representation of the structures: (left) double-layer monomer intercalating conformation of aniline/HNb_3O_8; (right) single-layer polymer intercalating conformation of PANI/HNb_3O_8.

(Scheme 1, right) and comparable with the published values of ~ 4.2 Å in PANI/UO_2PO_4 and PANI/$MnPS_3$, and ~ 7.0 Å in PANI/V_2O_5, PANI/MoO_3, and PANI/FeOCl, etc.[11–17]

In various polymerization processes, different interlayer heights of the nanocomposites were achieved. This indicates that the included angle between the plane of $Nb_3O_8^-$ slab and the aromatic rings of PANI is not the same, corresponding to the different polymerization mechanisms of the interlayered aniline monomers. It is commonly thought that the polymerization mechanism of bulk PANI in a solution involves two cation radicals reacting with each other to form a polymeric chain.[12,25]

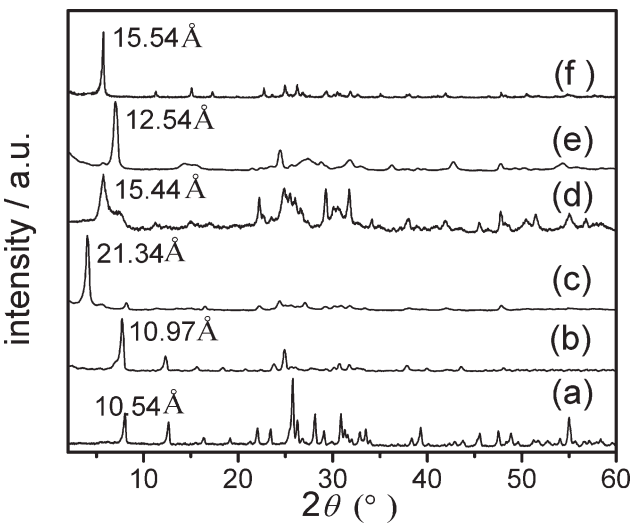

Figure 2 XRD patterns of (a) KNb_3O_8, (b) HNb_3O_8, (c) AnHNb, (d) PaniHNb-NH_4^+, (e) PaniHNb-Fe^{3+}, and (f) PaniHNb-MW.

Most of the observations related to the mode of oxidation (microwave vs. chemical oxidant) can easily be explained taking into account that microwave will be present in the sample instantaneously almost everywhere, chemical oxidant will slowly diffuse inside. In this work, since the chemical oxidant cannot easily diffuse into the limited interlayer space of HNb_3O_8, the formation of PANI starts with the formation of anilinium cation radicals at the edge of the AnHNb particles. Then, the anilinium cation radical reacts with the adjacent nucleophilic aniline to form a dimer radical, and continuously the chain growth reaction goes into the inner of the interlayers until a high-molecular-weight polymer is formed. The formation of anilinium cation radical is the rate-determining step.[26] Only a few cation radicals can be formed and initiate the polymerization from the outer to the inner within the interlayers, corresponding to the experimental phenomenon that the initiation time needed for the formation of nanocomposites PANIHNb-NH_4^+ and PANIHNb-Fe^{3+} is more than 6 h. During the chain growth, the reorientation and/or extrusion of PANI oligomers from the interlayers

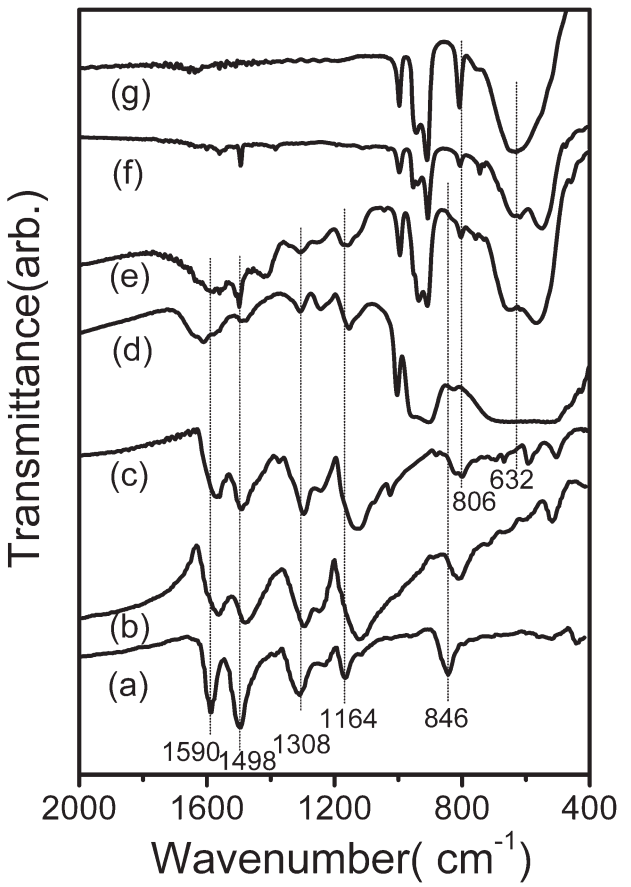

Figure 3 FTIR spectra of (a) bulk PANI base (dedoped by $NH_3 \cdot H_2O$), (b) bulk PANI salt (doped by 1.0*M* HCl), (c) PANIHNb-NH_4^+, (d) PANIHNb-Fe^{3+}, (e) PANIHNb-MW, (f) AnHNb, and (g) KNb_3O_8.

cause a part of aniline to be deintercalated[‡], and finally a single layer of PANI is formed.

On the contrary, because of the penetrating character of microwave irradiation, more inner aniline monomers within the interlayers can be simultaneously excited to form cation radicals during a relatively short time. The chain of PANI can grow both from inner and outer of the interlayer. The layered transition metal oxide could act as a catalyst to some extent, and the aniline molecules absorbed on the acidic inorganic slabs would be polymerized. During the polymerization, a part of aniline monomer is evaporated from the interlayers by the heat produced in the polymerization reaction and microwave irradiation, and finally the remaining aniline monomers are polymerized to form a single layer of PANI between the layers.

[‡]The deintercalated aniline monomers could be oxidized in the solution, but their concentration was too low to grow PANI, and only soluble oligomers with various lengths or anilinium ions were formed. After the polymerization, the solution washed out of the product showed a purple color, and the color became weak after several washings.

Infrared spectroscopy studies

Chemical oxidation and microwave irradiation treatment of the aniline-intercalated composite are accompanied with changes in the FTIR spectra (Fig. 3). For example, the vibrations of $Nb_3O_8^-$ in AnHNb are similar to those in KNb_3O_8. The octahedral vibrations of NbO_6 in KNb_3O_8 appear at 997.5, 909.6, and 807.9 cm^{-1}, and the absorption bands around 700 and 600 cm^{-1} are believed to be the vibrations of the corner-shared NbO_6 octahedron.[27] However, after the intercalated aniline monomers are polymerized, an obvious shift is observed in the PANI/HNb_3O_8 nanocomposites prepared by different polymerization methods because of the different strengths of interaction between PANI and layered host.

Compared with the characteristic IR absorptions (1590, 1498, 1308, 1164, and 846 cm^{-1}) of PANI base, the IR absorptions of bulk PANI salt (doped by HCl) are shifted to 1564, 1482, 1294, 1120, and 807 cm^{-1}, respectively.[28] These characteristic peaks of PANI also appear in the nanocomposites (PANIHNb-NH_4^+, PANIHNb-Fe^{3+}, and PANIHNb-MW), indicating that PANI is formed within the layers. The differences in the intensity and shifted position of these peaks in the nanocomposites can be ascribed to the particular orientation and protonation of PANI within the confined proton-rich space of HNb_3O_8. These differences also present some useful information about the doping level and degree of oxidation of the interlayered PANI. First, the protons of layered host have a relatively lower doping ability than the inorganic acid, because the interlayered protons simultaneously suffer the interaction of the negative $Nb_3O_8^-$ slabs and that of PANI. Second, different conformations of PANI molecules are formed between the confined spaces after polymerization initiated either in aqueous phase by using chemical oxidants or in solid phase by microwave irradiation. Thus, different strengths of interaction between the interlayered PANI molecules and inorganic slabs are revealed in the shifted FTIR vibrations. For example, the stretching vibration of quinoid rings appears at 1564 cm^{-1} in PANI salt, and this vibration is shifted to 1565, 1586, and 1610 cm^{-1} in PANIHNb-NH_4^+, PANIHNb-MW, and PANIHNb-Fe^{3+}, respectively. The vibrations of PANIHNb-Fe^{3+} shift more obviously than those of PANIHNb-NH_4^+ and PANIHNb-Fe^{3+}, because PANI is formed within the narrowest interlayers and has a relatively stronger interaction with the $Nb_3O_8^-$ slabs in PANIHNb-Fe^{3+}.

Morphology and structure of nanocomposites

SEM and TEM images of the layered host KNb_3O_8, HNb_3O_8, and the corresponding nanocomposites (AnHNb, PANIHNb-NH_4^+, PANIHNb-Fe^{3+}, and

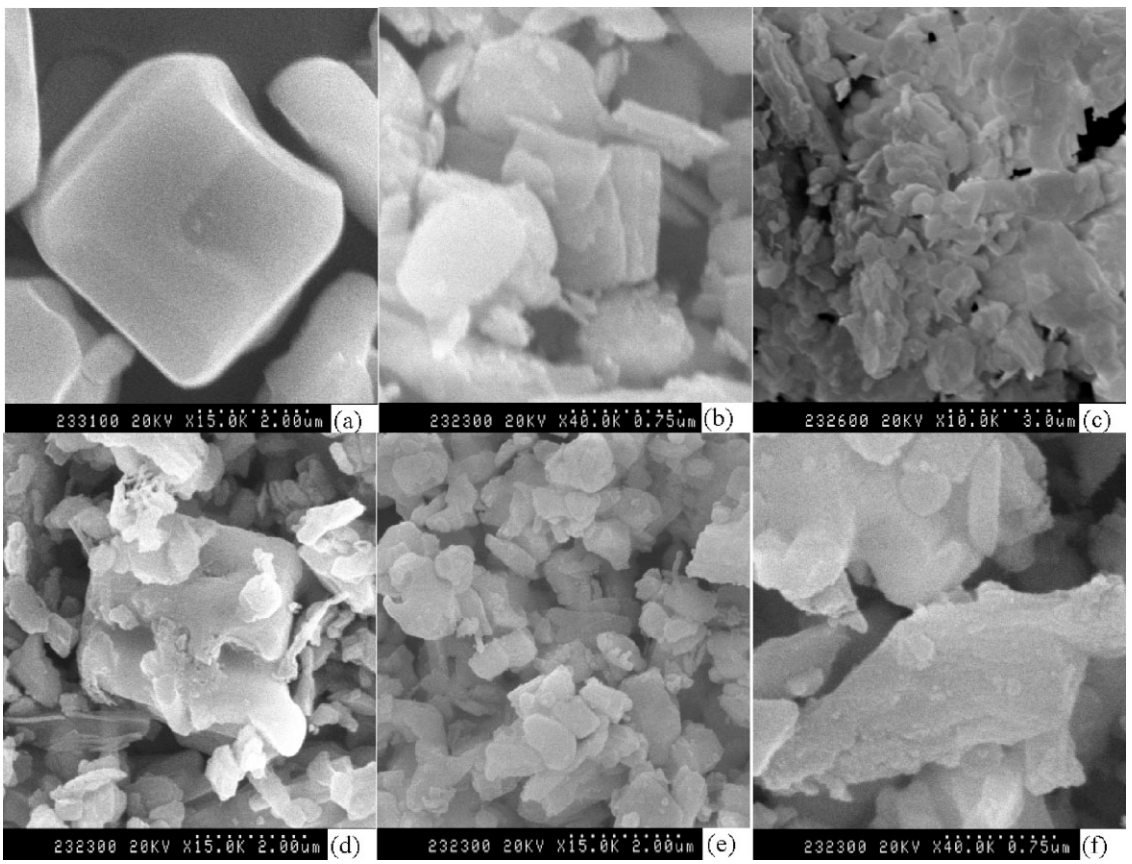

Figure 4 SEM images of (a) KNb_3O_8, (b) HNb_3O_8, (c) AnHNb, (d) PaniHNb-NH_4^+, (e) PaniHNb-Fe^{3+}, and (f) PaniHNb-MW.

PANIHNb-MW) are shown in Figures 4 and 5, respectively. Compared with the large ordered crystals of KNb_3O_8, HNb_3O_8 shows small crystals ($\sim$ 0.6 μm) and a little disorder on the edge of particles due to the proton exchange. As the monomer aniline is inserted and a bilayer arrangement of aniline molecules is formed within the interlayers of HNb_3O_8, the thin-sheet structure appears due to the large expansion of the interlayer distance [Fig. 5(a)]. After polymerization of the interlayered aniline, the crystal morphology of nanocomposites PANIHNb-NH_4^+, PANIHNb-Fe^{3+}, and PANIHNb-MW is very similar, but it is different from that of AnHNb particles [Figs. 4(d–f) and 5]. It is also possible to notice that the morphology of PANI/HNb_3O_8 nanocomposites is more similar to that of the layered host HNb_3O_8 [Fig. 4(b)] when compared with the aggregated ball-like morphology of the pure PANI prepared by the same method. This result suggests that the polymerization occurs mainly between the inorganic layers.

As shown in TEM images, the surfaces of nanocomposites are continuous and relatively homogeneous. The layered nature can be clearly observed in Figure 5. This is consistent with a typical topotactic intercalation in which the layer structure and morphology are preserved after intercalation and polymerization. Most of the images can be interpreted as overlapped sheets (Fig. 5). However, in SEM images [Fig. 4(d–f)], the surface of PANI/HNb_3O_8 nanocomposite particles is rougher than that of HNb_3O_8 and AnHNb, having many microcracks and some exfoliated sheets, because the exothermic polymerization leads to the shrinkage of lamellar structure. Moreover, as the PANI chains extend from the interlayers and link with each other among the adjacent crystals,[28] the nanocomposite crystals are aggregated and their sizes are larger than those of HNb_3O_8 and AnHNb [Fig. 4(b–f)].

Cyclic voltammetry and electroactivity of nanocomposites

CV experiments are always done to test the electroactivity of nanocomposites. The GCE was previously tested in different pH of HCl solutions before the sample was drop-coated on it, and it presented no redox behavior in the potential range studied. To assure the diffusion of solution into the interlayer space and to permit a better ionic exchange, the working electrode coated with the nanocomposite was immersed in the electrolyte solution for 30 min prior to the measurement.[29]

For the dedoped nanocomposite PANIHNb-NH_4^+, the similar redox behavior is shown in Figure 6 and

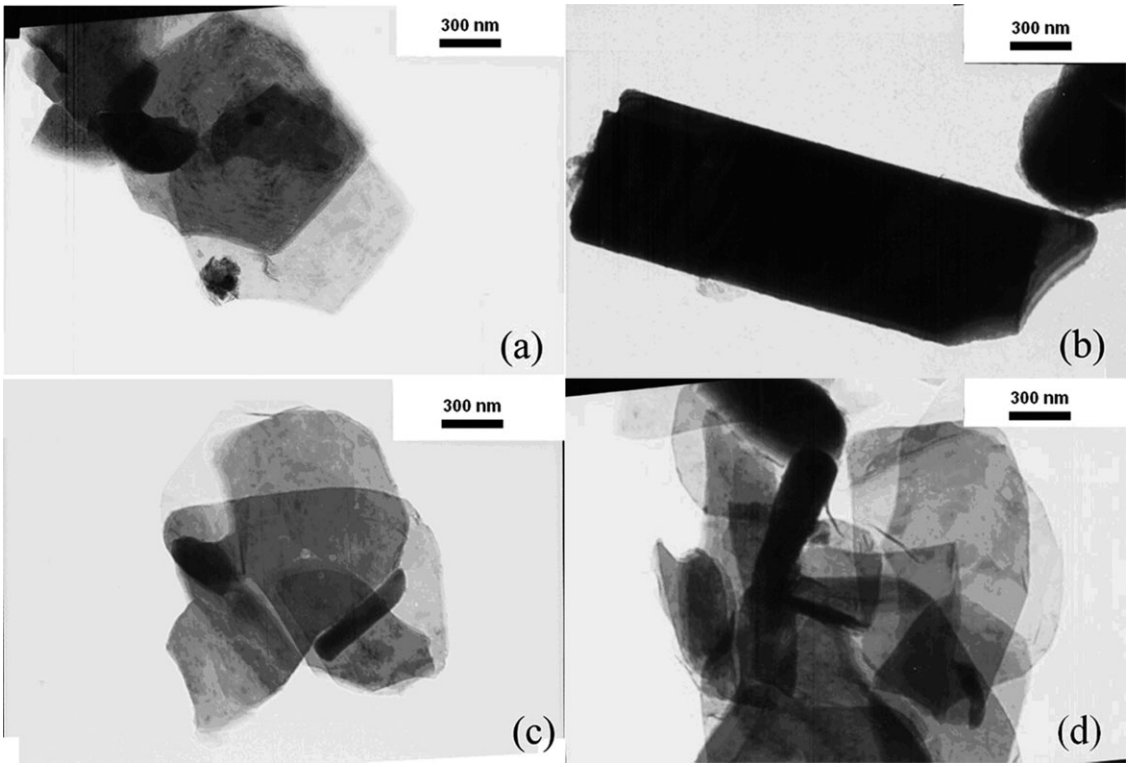

Figure 5 TEM images of (a) AnHNb, (b) PaniHNb-NH_4^+, (c) PaniHNb-Fe^{3+}, and (d) PaniHNb-MW.

indicated the diffusion control in different pH solution. There are two oxidation peaks observed at 0.24 and 0.48 V for the sample PANIHNb-NH_4^+ (dedoped by $NH_3{\cdot}H_2O$) in low-pH HCl solution [Fig. 6(a)]. As the pH value of the solution is increased gradually, the oxidation peaks merge to show only one broad peak at 0.37 V. This redox behavior is similar to that reported previously.[29,30] The peak around 0.37 V is ascribed to the overlapping of two redox processes of PANI normally found in acid conditions, that is, transition between the fully reduced leucoemeraldine base (LEB) form and half-oxidized EB form, and that between the EB form and fully oxidized pernigraniline base (PNB) form. The CV of dedoped PANIHNb-NH_4^+ measured in pH = 3 HCl solution reveal that the peak current is increased linearly with the scan rate [Fig. 6(b)], indicating a good ability of ions insertion/deinsertion between the layers. The redox behavior of nanocomposites may originate from the fact that the layered host provides a two-dimensional channel for the conducting carrier.

The redox peaks of nanocomposites are discussed based on the known models of pure PANI. A model that takes into account the elementary steps occurred in PANI was reported earlier by Peter and coworkers.[31] It is well known that PANI exists in three well-defined oxidation states: leucoemeraldine, emeraldine, and pernigraniline. In the leucoemeraldine state, all the nitrogen atoms are amines, whereas in pernigraniline, the nitrogen atoms are imines. The amine/imine ratio in emeraldine is ~ 1. The emeraldine can be converted between its base and salt forms, depending on the pH value. The first oxidation peak around $E_{SCE} = 0.24$ V can be assigned to the transition between leucoemeraldine state and emeraldine salt, and the second around $E_{SCE} = 0.48$ V to the transition between emeraldine salt and pernigraniline state.[32,33] The EB form is in equilibrium with its protonated ES form. Any change in the surrounding pH value will cause a change in the equilibrium forms of PANI within the grafting structure and a shift in voltammetric activity [as shown in Fig. 6(a)]. When EB is formed within the negative layers, more protons are needed to dope PANI and to balance the negative charge of the inorganic slabs simultaneously. However, this process is fast. On the contrary, when the protonated PANI is reduced, the strong interaction among protons, PANI molecules, and negative slabs decreases the elimination rate of protons. However, this process is slow. As demonstrated in the experimental facts, the anodic peak currents are relatively higher than the cathodic peaks (Fig. 6), indicating that the elimination rate of protons in the anodic process is greater than the addition rate of protons in the cathodic process.[33,34]

CONCLUDING REMARKS

Layered transition metal oxide HNb_3O_8 is a good compound for intercalation reactions. Monomers of

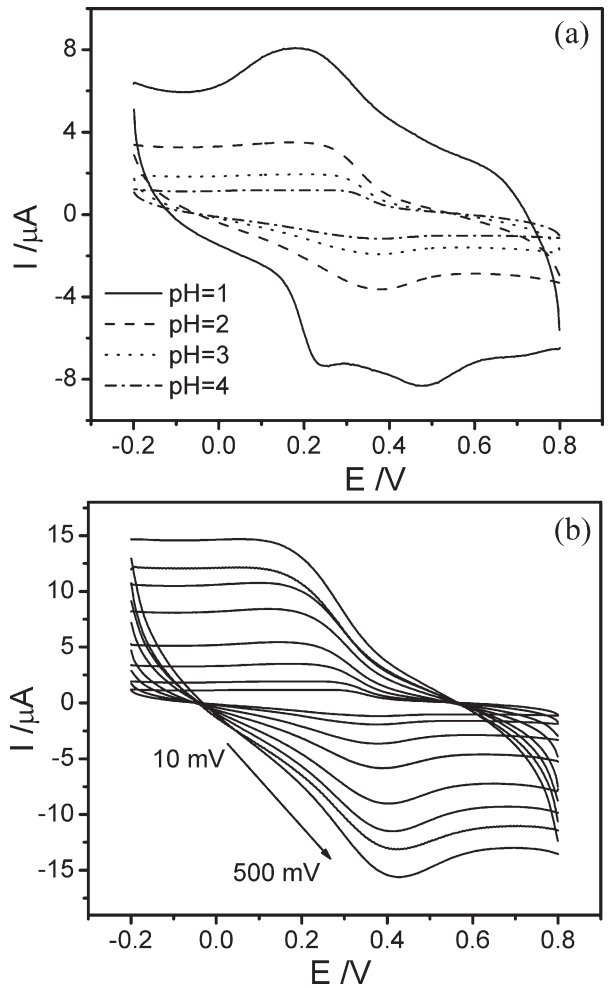

Figure 6 Cyclic voltammograms of PaniHNb-NH_4^+ dedoped with $NH_3{\cdot}H_2O$ measured in (a) different pH HCl solutions (scan rate was 50 mV s^{-1}) and (b) pH = 3 HCl solution, at scan rates of 10, 20, 50, 100, 200, 300, 400, and 500 mV s^{-1}.

aniline can be intercalated by the acid/base reaction. After the *in situ* polymerization, a single-layer arrangement of PANI is formed between the inorganic slabs, and the formed PANI demonstrated a much narrower molecular weight distribution than bulk PANI. Within the confined layer space, the polymerization initiated by chemical oxidants in solution involves that a few radicals are first formed on the edge of AnHNb microcrystals and then the chain growth reaction occurs from the outer to the inner of the interlayers. However, for the polymerization initiated by microwave irradiation in solid state, more radicals can be formed and PANI can be grown simultaneously on the edge and in the inner of the interlayers. The aromatic rings of the interlayered PANI could be parallel with or perpendicular to the inorganic slabs and the interlayered PANI molecules were ES and protonated by the protons of layered inorganic acid host. The ionic channel of the layered host is a unique function when compared with pure PANI, and thus the CV revealed that the properties of the layered host and the interlayer height have an effect on the redox behavior of the corresponding nanocomposites PANI/HNb_3O_8.

References

1. Cuentas-Gallegos, A. K.; Lira-Cantu, M.; Casan-Pastor, N.; Gomez-Romero, P. Adv Funct Mater 2005, 15, 1125.
2. Van Hoang, H.; Holze, R. Chem Mater 2006, 18, 1976.
3. Pang, S. P.; Li, G. C.; Zhang, Z. K. Macromol Rapid Commun 2005, 26, 1262.
4. Yang, G.; Hou, W. H.; Sun, Z. Z.; Yan, Q. J. J Mater Chem 2005, 15, 1369.
5. Karatchevtseva, I.; Zhang, Z.; Hanna, J.; Luca, V. Chem Mater 2006, 18, 4908.
6. Qiu, Y.; Gao, L. J. Phys Chem B 2005, 109, 19732.
7. Li, X. G.; Lü, Q. F.; Huang, M. R. Chem Eur J 2006, 12, 1349.
8. Fischer, J. E.; Zhu, Q.; Tang, X.; Scherr, E. M.; MacDiarmid, A. G.; Cajipe, V. B. Macromolecules 1994, 27, 5094.
9. Huang, J.; Virji, S.; Weiller, B.; Kaner, R. B. Chem Eur J 2004, 10, 1314.
10. Petkov, V.; Parvanov, V.; Trikalitis, P.; Malliakas, C.; Vogt, T.; Kanatzidis, M. G. J Am Chem Soc 2005, 127, 8805.
11. Park, N. G.; Ryu, K. S.; Park, Y. J.; Kang, M. G.; Kim, D. K.; Kang, S. G.; Kim, K. M.; Chang, S. H. J Power Sources 2002, 103, 273.
12. Shao, K.; Ma, Y.; Chen, Z. H.; Ji, X. H.; Yang, W. S.; Yao, J. N. Chem Lett 2002, 322.
13. Hix, G. B.; Maddocks, X. C.; Harris, K. D. M. Polyhedron 2000, 19, 765.
14. Wang, L.; Rocci-Lane, M.; Brazis, P.; Kannewurf, C. R.; Kim, Y. I.; Lee, W.; Choy, J. H.; Kanatzidis, M. G. J Am Chem Soc 2000, 122, 6629.
15. Shim, I. W.; Oh, W. S.; Jeong, H. C.; Seok, W. K. Macromolecules 1996, 29, 1099.
16. Goddard, Y. A.; Vold, R. L.; Hoatson, G. L. Macromolecules 2003, 36, 1162.
17. Cho, M. S.; Choi, H. J.; Ahn, W.-S. Langmuir 2004, 20, 202.
18. Quillard, S.; Louarn, G.; Lefrant, S.; MacDiarmid, A. G. Phys Rev B 1994, 50, 12496.
19. MacDiarmid, A. G.; Chiang, J. C.; Richter, A. F.; Epstein, A. J Synth Met 1987, 17, 285.
20. Takagaki, A.; Sugisawa, M.; Lu, D.; Kondo, J. N.; Hara, M.; Domen, K.; Hayashi, S. J Am Chem Soc 2003, 125, 5479.
21. Schaak, R. E.; Mallouk, T. E. Chem Mater 2002, 14, 1455.
22. Liu, J. F.; Li, X. L.; Li, Y. D. J Cryst Growth 2003, 247, 419.
23. Dion, M.; Ganne, M.; Tournoux, M. Mater Res Bull 1981, 16, 1429.
24. Amicangelo, J. C.; Rosenthal, G. L.; Leenstra, W. R. Chem Mater 2003, 15, 390.
25. Klavetter, F.; Cao, Y. Synth Met 1993, 55, 989.
26. Percec, V.; Hill, D. H. Cationic Polymerization: Mechanism, Synthesis, and Applications, Matyjaszewski, K.; Pugh, C., Eds.; Marcel Dekker: New York, 1996; p 646.
27. de Andrade, J. S.; Pinheiro, A. G.; Vasconcelos, I. F.; Sasaki, J. M.; de Paiva, J. A. C.; Valente, M. A.; Sombra, A. S. B. J Phys: Condens Matter 1999, 11, 4451.
28. Wu, Q.; Xue, Z.; Qi, Z.; Wang, F. Polymer 2000, 41, 2029.
29. Tian, S. J.; Baba, A.; Liu, J. Y.; Wang, Z. H.; Knoll, W.; Park, M.-K.; Advincula, R. Adv Funct Mater 2003, 13, 473.
30. Lu, W.; Smela, E.; Adams, P.; Zuccarello, G.; Mattes, B. R. Chem Mater 2004, 16, 1615.
31. Kalaji, M.; Nyholm, L.; Peter, L. M. J Electroanal Chem 1991, 313, 271.
32. Huang, W.-S.; Humphrey, B. D.; MacDiarmid, A. G. J Chem Soc Faraday Trans 1986, 82, 2385.
33. Shreepathi, S.; Holze, R. Chem Mater 2005, 17, 4078.
34. Jiang, R.; Dong, S. Synth Met 1988, 24, 255.